

Experimental evidence for an intermediate phase in the multiferroic YMnO_3

G. N. N. enert¹, M. Pollet², S. Marinell³, G. R. Blake¹, A. Meetsma¹
and T. T. M. Palstra¹

¹Solid State Chemistry Laboratory, Zernike Institute for Advanced Materials,
University of Groningen, Nijenborg 4, 9747 AG Groningen, The Netherlands

²ICM CB - CNRS Physico-Chimie des Oxydes Conducteurs, 87 Avenue du Docteur
Schweitzer 33608 Pessac Cedex France

³Laboratoire CRISMAT, UMR CNRS ENSICAen -14050 Caen Cedex 4 France

Abstract.

We have studied YMnO_3 by high-temperature synchrotron X-ray powder diffraction, and have carried out differential thermal analysis and dilatometry on a single crystal sample. These experiments show two phase transitions at about 1100K and 1350K, respectively. This demonstrates the existence of an intermediate phase between the room temperature ferroelectric and the high temperature centrosymmetric phase. This study identifies for the first time the different high-temperature phase transitions in YMnO_3 .

PACS numbers: 61.10.Nz, 77.80.Bh

1. Introduction

In typical ferroelectrics the creation of an electric dipole moment involves a charge transfer between empty d-shell metal ions and occupied 2p orbitals of oxygen. This mechanism of ferroelectricity precludes magnetic moments and magnetic order. YMnO_3 is part of a class of materials that exhibit both electric and magnetic orders, called multiferroics. The coexistence of ferroelectricity and magnetic order allows the manipulation of electric and magnetic moments by magnetic and electric fields, respectively [1]. In multiferroics, the charge transfer from the 2p orbitals towards the transition metal ion is not relevant due to the partially filled nature of the d-shell. Indeed, in YMnO_3 the Mn-ion remains in the barycenter of its oxygen coordination. However, this charge transfer is allowed towards the empty d-shell of the rare-earth and creates two dipoles of opposite sign resulting in a ferroelectric state [2]. Recent ab-initio calculations indicate that the ferroelectric state involves no charge-transfer, but is related to the tilting of the MnO_5 polyhedra [3]. However, there is no clear high-temperature structural information about this transition to clarify the origin of the ferroelectric state in this material. While a lot of effort is put in the search and design of new multiferroics, the nature of the mechanism of ferroelectricity and thus the nature of the coupling between the different degrees of freedom is still not well understood in YMnO_3 . We can distinguish two classes of antiferromagnetic ferroelectrics: T_N (Néel temperature) $> T_{FE}$ (critical temperature for ferroelectricity) and $T_N < T_{FE}$. For the first class, with compounds like RMn_2O_5 and $o\text{-RMnO}_3$ (orthorhombic), the mechanism of ferroelectricity can be understood phenomenologically by the existence of a gradient of the magnetization (incommensurate helicoidal spin structure) leading to a transverse polarization [4, 5]. The coexistence and strong coupling between ferroelectricity and incommensurate magnetism in $o\text{-RMnO}_3$ is related to Dzyaloshinskii-Moriya interactions [6]. For the second class, which includes $h\text{-RMnO}_3$ (hexagonal), the origin of ferroelectricity is not well understood since the Mn o -centering is not responsible for the ferroelectricity [3]. Moreover, the $h\text{-RMnO}_3$ is particularly interesting due the high polarization at room temperature ($P_S \approx 5.5 \text{ C/cm}^2$). The $h\text{-RMnO}_3$ exhibit $T_{FE} \approx 1000 \text{ K}$ and $T_N \approx 100 \text{ K}$. Despite this difference, recent studies of $h\text{-RMnO}_3$ show that the ferroelectric and antiferromagnetic order parameters are coupled [7, 8, 9, 10].

YMnO_3 adopts the centrosymmetric space group $P6_3/mmc$ in its high temperature paraelectric state and the polar space group $P6_3cm$ at room temperature with a unit cell that is tripled in volume (the a and b axes are lengthened by a factor of $\sqrt{3}$). However, the ferroelectric transition temperatures reported in the literature fall into two distinct groups, and when taken together, previous studies of YMnO_3 suggest that there are not one but two distinct phase transitions above room temperature [11]. However, these phase transitions have never both been observed in a single experiment. Moreover it has consistently been reported that the ferroelectric transition of YMnO_3 occurs at 933K, and not higher as claimed by Abraham et al. [12]. If an Intermediate Phase (IP) exists,

its symmetry and nature have not yet been determined.

In recent years, two structural studies have been carried out on $h-RMnO_3$ powder in the high temperature regime either by synchrotron or by neutron diffraction [3, 14]. Both experiments failed to observe any structural phase transitions even though measurements were performed up to 1000K for $R = Y$ (synchrotron), up to 1300K for $R = Lu$, 1100K for $R = Yb$ and 1400K for $R = Tm$ (neutron). Lonka et al. realized using symmetry arguments that two high temperature phase transitions are necessary [14]. Therefore, they proposed an antiferroelectric IP having the same symmetry as the room temperature phase ($P6_3cm$). We believe that the absence of observations of phase transitions in these two recent studies, contradicting older results, has caused confusion regarding the high temperature behavior of $YMnO_3$. The succession of three states has thus far been only theoretically incorporated in investigations of the origin of the ferroelectric state [3, 15]. The aim of this paper is to prove experimentally the existence of an IP in $YMnO_3$. Furthermore, we will show that our data are in agreement with previous experimental observations.

First, we report the room temperature structure of a high quality single crystal. Using dilatometry and differential thermal analysis, we demonstrate in a single experiment the existence of an intermediate phase stable between T_{C1} and T_{C2} . In addition, based on synchrotron X-ray powder diffraction, we confirm the existence of the paraelectric phase above T_{C2} with the $P6_3/mmc$ symmetry. Finally, we discuss the differences in transition temperatures between our results and earlier reports in the light of single crystal quality.

2. Experimental Techniques

$YMnO_3$ powder was synthesized by reacting stoichiometric amounts of Y_2O_3 (4N) and MnO_2 (3N metal basis) in nitrogen atmosphere at 1200 C for 10h. The powder was reground and resintered once under the same conditions to improve crystallinity. A single crystal was grown from the powder in air by the Floating Zone technique using a four mirror furnace. The good crystallinity of the crystal was confirmed by Laue diffraction.

We have carried out an additional high temperature synchrotron X-ray experiment on the beam line ID 31 at ESRF (Grenoble, France) using a wavelength of 0.3 Å. The powder sample was placed in a spinning Pt capillary which was heated by means of a three mirror furnace. The temperature control was monitored by the position of the Pt peaks with a feedback system to compensate for the aging of the lamps. Rietveld refinements of the data were carried out using the GSAS software package [6].

In order to check the quality of our single crystal, we carried out a full data set collection at room temperature. A black crystal with approximate dimensions of 0.14 × 0.12 × 0.04 mm was measured at room temperature on a Bruker SMART APEX CCD diffractometer. Intensity measurements were performed using graphite monochromatic Mo-K α radiation. The λ unit cell was obtained from the xyz centroids

of 1743 reflections after integration. Intensity data were corrected for Lorentz and polarization effects and for absorption [17]. The program suite SHELXTL was used for space group determination assuming an inversion twin [18].

The differential thermal analysis (DTA) was carried out in a flow of nitrogen using a SDT 2960 of TA Instruments between room temperature and 1473K with a ramp of 5K/m in. We used a crushed single crystal for this experiment in a platinum pan.

The dilatometry measurements were carried out in static air using a SETARAM TMA 92 dilatometer. The temperature ramp was 1 K/m in starting from room temperature to 1473K. A load of 10 g was applied on the single crystal to optimize the signal to noise ratio. The choice of this load was based on several trial runs. The sample used was cut in a rectangular shape, but not oriented along a particular crystallographic orientation. The single crystal was protected from the alumina parts using platinum sheets. All measurements were corrected for the blank signal (alumina + platinum).

3. Results-Discussion

The refined atomic coordinates and isotropic displacement parameters of our crystal at room temperature are presented in Table 1. The crystal contains inversion twins as a natural consequence of the polar structure. The structure is very similar to that previously reported [13]. However, there is a significant difference in the unit cell volume of our crystal compared with the structures of the single crystals grown from Bi_2O_3 flux (see Table 2), even when experimental uncertainty is taken into account. We will discuss later the possible origin of such difference and its consequence for the ferroelectric transition temperature.

Atoms	x	y	z	$U_{\text{eq}} (\text{\AA}^2)$
Y_1	0	0	0.7711 (2)	0.0056 (5)
Y_2	1/3	2/3	0.73038 (-)	0.0060 (3)
Mn	0.6672 (5)	0	0.4976 (2)	0.0059 (5)
O_1	0.697 (1)	0	0.661 (1)	0.010 (2)
O_2	0.353 (1)	0	0.8352 (9)	0.005 (2)
O_3	0	0	0.973 (2)	0.008 (3)
O_4	1/3	2/3	0.515 (1)	0.010 (3)

Table 1. Atomic coordinates of a single crystal YMnO_3 grown by the Floating Zone Technique from data collected at room temperature. The cell parameters are $a = 6.1469(6)\text{\AA}$ and $c = 11.437(1)\text{\AA}$ (space group $P6_3cm$, $wR(F^2) = 8.45\%$ and $R(F) = 3.43\%$). In parentheses, we indicate the standard uncertainty. The z coordinate of Y_2 was fixed due to the lack of a center of symmetry.

In Fig. 1, we show the temperature dependence of the dilatometric response of an unoriented single crystal of YMnO_3 . We observe clearly two anomalies while heating. The first anomaly, denoted T_{C1} , appears at about 1125K and the second anomaly

Reference	a (Å)	c (Å)
Ref. 19	6.145	11.42
Ref. 20	6.1387 (3)	11.4071 (3)
Ref. 21	6.125 (1)	11.41 (1)
This work	6.1469 (6)	11.437 (1)

Table 2. Comparison of the lattice parameters between single crystals grown from a Bi_2O_3 flux and this work.

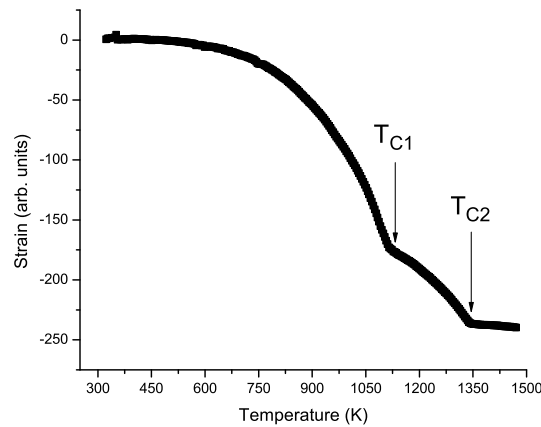


Figure 1. Dilatometry measurement of an unoriented single crystal of YMnO_3 . The arrows indicate the two transition temperatures T_{C1} and T_{C2} .

appears at $T_{C2} = 1350\text{K}$. These transitions are also observed in our DTA experiment, shown in Fig. 3, where we notice anomalies at about 1100K for T_{C1} and at 1350K for T_{C2} .

We had a closer look at the temperature dependence of the thermomechanical analysis (TMA) response close to T_{C2} . In Fig. 2, we show a zoom of the TMA response close to T_{C2} , which is linear below about 1340K . While measuring the TMA response, one measures the strain which usually plays the role of a secondary order parameter during a phase transition. Indeed, we know that the transition from the HT phase to the IP could involve some strain as a secondary order parameter [22]. The linear dependence on temperature of the TMA response suggests that the transition at T_{C2} is of 2nd order.

In order to clarify the nature of the two phase transitions, we carried out a DTA experiment on a crushed single crystal under N_2 atmosphere. The results are presented in Fig. 3. We notice a small anomaly at T_{C1} and a larger one at T_{C2} . The differentiation between 2nd order and 1st order phase transitions using DTA remains a non-straightforward task [23]. While we observe a large peak at about 1350K , the DTA anomaly at about 1100K is small. This suggests that this transition at 1350K requires significantly more energy than the one from IP towards the RT phase

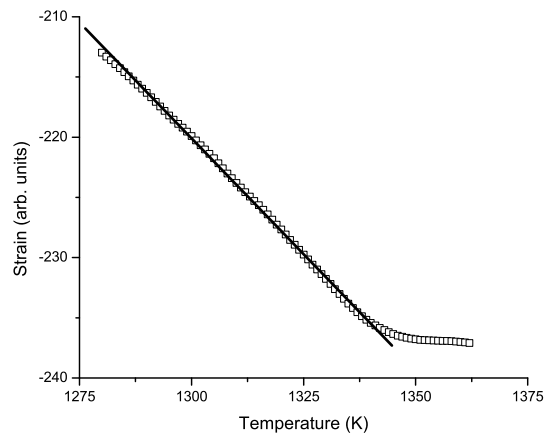


Figure 2. Linear temperature dependence below T_{C2} of the thermomechanical analysis.

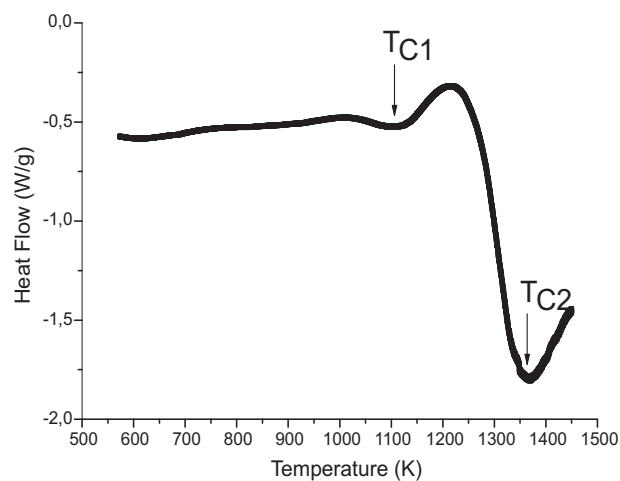


Figure 3. Differential Thermal Analysis of a crushed single crystal of YMnO_3 . The measurement was carried out in a N_2 atmosphere with a rate of $5\text{K}/\text{m}$ in. The arrows indicate the ferroelectric transition temperature T_{C1} and the tripling of the unit cell T_{C2} .

We further investigated YMnO_3 using synchrotron X-ray powder diffraction. We collected data at several temperatures, concentrating on the range $950\text{K} - 1475\text{K}$. This is below and above the transition temperature T_{C2} observed in the dilatometry and DTA experiments. We present the measured cell parameters in Fig. 4.

In Fig. 4, we can clearly see an anomaly around 1350K characterizing the transition towards the high-temperature paraelectric phase with $P6_3/mmc$ symmetry [14, 19]. The transition at T_{C2} is confirmed by the disappearance of the (206) reflection, which is characteristic of the tripled unit cell, as shown in Fig. 5.

We summarize in Table 3 the atomic coordinates in the high temperature centrosymmetric phase $P6_3/mmc$ at 1373K . A physically meaningful model could be

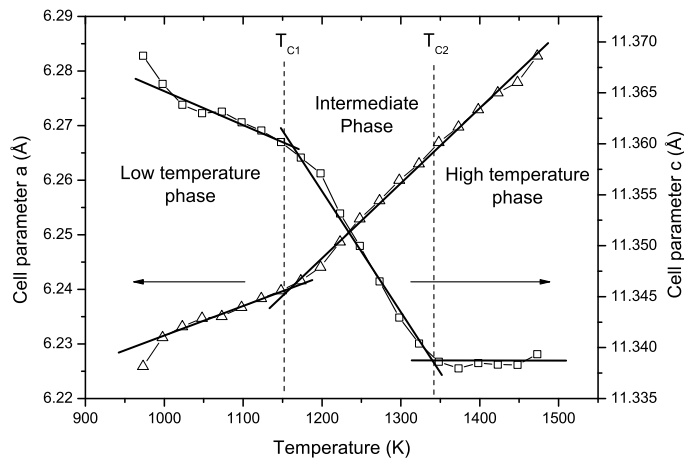


Figure 4. Cell parameters obtained from a powder sample at the ID 31 beam line at ESRF with $P6_3cm$ symmetry. The high temperature data above T_{C2} have the symmetry $P6_3/mmc$ and its cell parameters are $a' = \frac{a}{3}$ and $c' = c$.

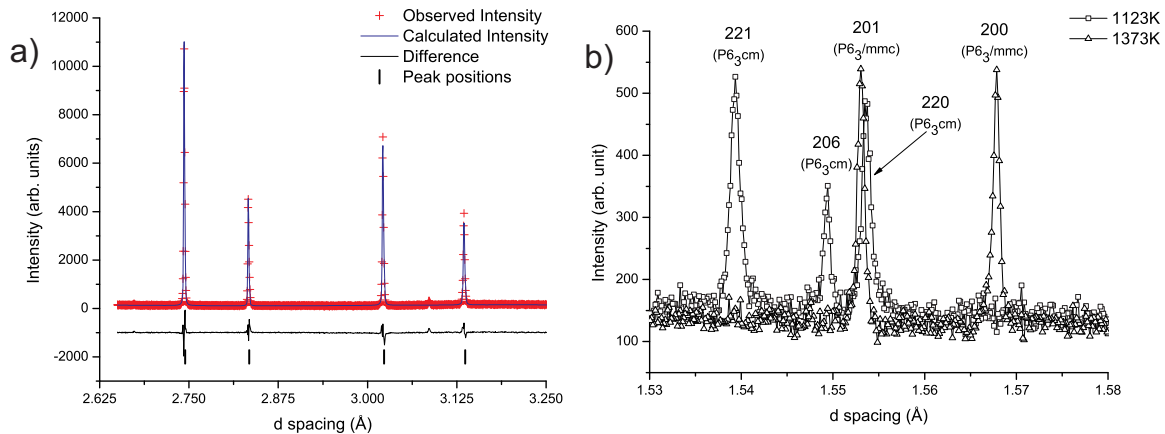


Figure 5. a) Portion of the Rietveld refinement using the $P6_3/mmc$ symmetry at 1373K, b) Disappearance of the (206) reflection as function of temperature determined by X-ray synchrotron diffraction. This evidences the transition towards the $P6_3/mmc$ symmetry.

reached only by constraining all the U_{iso} of the different atoms to be equal.

We observe that the transition at T_{C2} in Fig. 4 does not show any discontinuity. Thus in the light of the results of dilatometry data, DTA and diffraction data, we interpret both transitions at T_{C1} and at T_{C2} as second order phase transitions. We notice that the transition at T_{C1} is more obvious in the dilatometry experiment than in the synchrotron X-ray powder data. We observe that the transition at T_{C1} in the powder sample appears to be broadened. This type of phenomenon is often seen in polycrystalline samples where different grains will undergo the transition at slightly

Atom	x	y	z	U_{iso}
Y	0	0	0	0.0270 (7)
Mn	1/3	2/3	1/4	0.0270 (7)
O ₁	0	0	1/4	0.0270 (7)
O ₂	1/3	2/3	0.0821 (8)	0.0270 (7)

Table 3. Atomic coordinates determined by X-ray synchrotron Rietveld refinement at 1373K in the $P6_3/mmc$ symmetry. Cell parameters: $a = 3.62178(2)$ Å and $c = 11.3379(2)$ Å.

different temperatures due to the effects of factors such as grain size, morphology and strain. Indeed a change in slope of the c cell parameter is seen in the vicinity of T_{c1} (see Fig. 4).

As we have already remarked, the unit cell for single crystals grown from a Bi_2O_3 flux is systematically smaller than for crystals grown by the floating zone technique. There are two possibilities to explain this difference: a significant amount of Bi could be incorporated in the structure and/or the amount of vacancies can be different in the crystal structure caused by the different growth techniques.

We expect that if Bi is incorporated into the structure, it will preferentially occupy the 7-fold coordinated yttrium site. This hypothesis can be disregarded for several reasons. First, Bi^{3+} has a larger Shannon radius than Y^{3+} : $r(\text{Bi}^{3+}) = 1.24$ Å (derived from the average between 6-fold coordination and 8-fold coordination) and $r(\text{Y}^{3+}) = 1.1$ Å [24]. Therefore, we expect an increase of the cell parameters. Second, we have carried out refinements of the occupation on both Y-sites using the dataset of van Aken et al. [20] and our data. We did not find any evidence for substitution of Y by Bi. Thus, we have no experimental evidence for the incorporation of Bi into the lattice.

The second possible explanation for the smaller unit cell of flux-grown crystals is the creation of vacancies. According to Abraham's [25], vacancies would also affect the ferroelectric transition temperature, which can be expressed as (in Kelvin):

$$T_{\text{FE}} = (\frac{1}{2}k) (\frac{z}{c})^2 \quad (1)$$

where $\frac{1}{2}k$ is a force constant, k is Boltzmann's constant and z is the largest displacement along the polar c axis between the ferroelectric phase and the paraelectric phase. This value is expressed in Å due to $z = (z_{\text{para}} - z_{\text{ferro}}) c$. The ratio $\frac{1}{2}k$ has been estimated as $2.00(9) \cdot 10^4 \text{ K Å}^{-2}$. According to equation 1, a decrease of T_{FE} implies a decrease of the force constant, the displacement of the rare earth $z_{\text{para}} - z_{\text{ferro}}$ and/or the c lattice parameter. It is obvious that defects can be responsible for such changes. For instance, an excess in yttrium ($\text{YMn}_{1-x}\text{O}_{3-3/2x}$) would certainly both decrease the c parameter (consistent with the observations) and lower $\frac{1}{2}k$. In the same way, impurities can lower T_{FE} . Experiments using alumina crucibles instead of platinum can easily result in $\text{YMn}_{1-x}\text{Al}_x\text{O}_3$. Such a substitution would again account for a small decrease in the c parameter. All of these suggestions need to be checked experimentally. We

note that the presence of oxygen vacancies within the structure is unlikely because they would lead to electrostatic repulsions between the cations, enlarging the unit-cell.

The expected dependence of T_{C1} on the concentration of vacancies can explain the discrepancies between the recent results of Lonkai and Katsufuji and those in the older literature. Both groups used powders whereas all previous studies were performed on single crystals grown from a Bi-ux. Both experiments failed to observe a phase transition, except for $R = Tm$ where Lonkai et al. [14] observed the start of a transition, however without reaching the IP. Katsufuji et al. measured until 1000K for $YMnO_3$, synthesized in air, while our experiments show a transition at 1100K. For $R = Lu$ and $R = Yb$, neither Lonkai et al. [14] nor Katsufuji et al. [13] measured at sufficiently high temperatures to observe a phase transition. For the smaller rare-earths the ferroelectric transition is expected to be higher than for $R = Y$ [12]. Therefore, our work seems in agreement with previous literature, if one accepts that $YMnO_3$ grown in a B_2O_3 ux exhibits suppressed transition temperatures.

4. Conclusion

We provide experimental evidence for two high temperature phase transitions in $YMnO_3$ using dilatometry, DTA and synchrotron X-ray powder diffraction. This is the first proof in one single experiment for the existence of an intermediate phase in $YMnO_3$. We describe these transitions at T_{C1} and T_{C2} as being likely second order in nature. Above T_{C2} , we confirm the existence of a paraelectric phase with the $P6_3/mmc$ symmetry. We relate the higher transition temperatures of our crystal to the synthesis technique that we used. However, the nature of the intermediate phase remains to be investigated. Further experiments are in progress in order to give a full description of this system.

5. Acknowledgement

We thank M. Brunelli, C. V. Colin, A. J. C. Buum a and N. Mufti for technical support during the experiment at ESRF. The work was supported by the Dutch National Science Foundation NWO by the breedtestrategie programma of the Materials Science Center, MSC⁺. M.P. gratefully acknowledges the French Ministère de la Recherche et de la Technologie and the Délégation Régionale à la Recherche et à la Technologie, région Aquitaine, for financial support.

References

- [1] J. Wang, B. Neaton, H. Zheng, V. Nagarajan, S. B. O'gale, B. Liu, D. Viehland, V. Vaithyanathan, D. G. Schlom, U. V. Waghmare, N. A. Spaldin, K. M. Rabe, M. Wuttig, R. Ramesh, Science 299, 1719 (2003); T. Kimura, T. Goto, H. Shintani, K. Ishizaka, T. Arima and Y. Tokura, Nature 426, 55 (2003) and N. Hur, S. Park, P. A. Sharma, J. S. Ahn, S. Guha and S.-W. Cheong, Nature 429, 392 (2004)
- [2] The structure of $YMnO_3$ can be described by layers of edge-sharing trigonal bipyramids of oxygen surrounding Mn atoms. These layers are separated by layers of Y. The rare-earth atoms have a

non-conventional 7-fold coordination. A cooperative buckling of the MnO_5 trigonal bipyramids below T_{FE} displaces the Y^{3+} ions along the c axis. The displacements of the 2 symmetrically inequivalent Y ions in the unit cell are in opposite directions. Thus we call the polarized state of $YMnO_3$ a ferroelectric state (two opposite non-compensated polarizations).

- [3] B. van Aken, T.T.M. Palstra, A. Filippetti and N.A. Spaldin, *Nature Materials* 3, 164 (2004)
- [4] M. Mostovoy, *Phys. Rev. Lett.* 96, 67601 (2006)
- [5] H. Katsura, N. Nagaosa and A.V. Balatsky, *Phys. Rev. Lett.* 95, 57205 (2005)
- [6] I.A. Sergienko and E. Dagotto, *Phys. Rev. B* 73, 94434 (2006)
- [7] Z.J. Huang, Y. Cao, Y.Y. Sun, Y.Y. Xue, and C.W. Chu, *Phys. Rev. B* 56, 2623 (1997)
- [8] M.N. Iliev and H.-G. Lee, *Phys. Rev. B* 56, 2488 (1997)
- [9] M. Fiebig, Th. Lottermoser, D. Frohlich, A.V. Goltssev and R.V. Pisarev, *Nature* 419, 818 (2002)
- [10] B. Lorenz, A.P. Litvinchuk, M.M. Gospodinov, and C.W. Chu, *Phys. Rev. Lett.* 92, 87204 (2004)
- [11] Bertaut et al. *C.R. Acad. Sci. Paris*, 256, 1958 (1963); Bokov et al. *Sov. Phys. Solid State*, 5, 2646, (1964); Smolenskii et al. *J. Appl. Phys.*, 35, 915, (1964); I.G. Ismailzade and S.A. Kizhaev, *Sov. Phys. Solid State*, 70, 236 (1965); J.-C. Peuzin, *C.R. Acad. Sc. Paris*, 261, 2195-2197 (1965); Coeure et al. *Proceedings of the International Meeting on Ferroelectricity*, 1, 332 (1966); K. Lukaszewicz and J. Kanat-Kalicinska, *Ferroelectrics* 7, 81 (1974).
- [12] S.C. Abraham et al., *Acta Cryst. B* 57, 485, (2001)
- [13] T. Katsufuji, M. Masaki, A. Machida, M. Morimoto, K. Kato, E. Nishibori, M. Takata, M. Sakata, K. Ohoyama, K. Kitazawa, and H. Takagi, *Phys. Rev. B* 66, 134434 (2002)
- [14] T. Lonkai, D.G. Tomuta, U. Amann, J. Ihinger, R.W.A. Hendrikx, D.M. Tobben, and J.A. Mydosh, *Phys. Rev. B* 69, 134108 (2004)
- [15] C.J. Fennie and K.M. Rabe, *Phys. Rev. B* 72, 100103 (2005)
- [16] A.C. Larson and R.B. von Dreele, *General Structure Analysis System GSAS*, Los Alamos National Laboratory Report No. LAUR 86-748, 1994 (unpublished).
- [17] Sheldrick, G.M. (2001). *SADABS. Version 2. Multi-Scan Absorption Correction Program*. University of Göttingen, Germany
- [18] Bruker (2000). *SMART, SAINT, SADABS, XPREP and SHELXTL/NT. Area Detector Control and Integration Software*. Smart Apex Software Reference Manuals. Bruker Analytical X-ray Instruments. Inc., Madison, Wisconsin, USA
- [19] K. Lukaszewicz et al., *Ferroelectrics* 7, 81 (1974)
- [20] B. van Aken, A. Meetsma and T.T.M. Palstra, *Acta Cryst. C* 57, 230, (2001)
- [21] H.L. Yakel, W.C. Kochler, F. Bertaut, E. Forrat, *Act. Cryst.* 16, 957 (1963)
- [22] *The Landau Theory of Phase Transitions*, J.-C. Toledano and P. Toledano; World Scientific Publishing 1987
- [23] P. Navard and J.M. Haudin, *J. Thermal Analysis* 30, 61 (1985)
- [24] R.D. Shannon, C.T. Prewitt, *Acta Cryst. B* 26 1046 (1970); R.D. Shannon, C.T. Prewitt, *Acta Cryst. B* 25, 925 (1969)
- [25] S.C. Abraham, S.K. Kurtz and P.B. Jamieson, *Phys. Rev.* 172, 551 (1968)